The collapse of a mixed patch in stratified fluid

Bruce R. Sutherland,[a] Amenda N. F. Chow, and Tyler P. Pittman
Department of Physics and Department of Earth and Atmospheric Sciences, 238 CEB, University of Alberta, Edmonton, Alberta T6G 2G7, Canada

(Received 11 June 2007; accepted 24 October 2007; published online 29 November 2007)

Lock-release laboratory experiments are performed to examine the collapse of a localized mixed patch of fluid in a uniformly stratified ambient with constant buoyancy frequency, N. The intrusion speed is approximately $0.13NH_\ell$, in which H_ℓ is the depth of the mixed patch. This is consistent with the speed of intrusions released from a full-depth lock where $H_\ell = H$ is the depth of the ambient. The vertically propagating waves have frequency set by N ($\omega \simeq 0.7N$) and the horizontal wavelength, λ_x, is set by H_ℓ ($\lambda_x \simeq 1.5H_\ell$). The amplitude is found to scale as the depth of the mixed region cubed at small H_ℓ, and saturates at large $H_\ell \gtrsim 10$ cm due to nonlinear effects. © *2007 American Institute of Physics*. [DOI: 10.1063/1.2814331]

I. INTRODUCTION

Oceans and lakes typically are stably stratified meaning that their effective density increases with depth. For example, descending through the thermocline the temperature rapidly cools and, as a result, vertical motions are inhibited because they require work against buoyancy forces (e.g., see Gill[1]).

Localized mixing can nonetheless occur as a consequence of highly energetic surface motions, which are dominantly driven by surface wind stresses. In particular, transient events such as tropical storms and hurricanes have been observed to mix the surface waters down to depths of several hundred meters. If the mixing is relatively shallow, the layer may restratify through surface heating[2] or through horizontal turbulence.[3] However, deeply mixed fluid that does not adjust in this way, may end up spreading laterally about the depth of neutral buoyancy, propagating as an intrusion. An observation of such a phenomenon was noted by Gregg.[4] Mixing on relatively smaller scales can occur as a result of shear instability and interactions between internal waves that lead to breaking.[5] Because such events occur rapidly, the mixed patch is also expected to collapse as an intrusion, though there are few observations of such transient events.

The work presented here focuses upon some aspects of the process of restratification that follows a mixing event. Specifically, it measures the rate at which a mixed patch intrudes horizontally into the surrounding stratified ambient and it examines the coupling between this intrusion and vertically propagating internal waves. The focus is upon the dynamics over short times during the collapse and so the effects of background rotation are ignored.

Intrusions are a special manifestation of gravity currents, which are flows that propagate horizontally due to horizontal density (and hence horizontal pressure) variations.[6,7] The evolution of gravity currents have often been examined by way of "lock-release" laboratory experiments. In these a patch of fluid of one density in a "lock" is separated initially by a gate from the ambient fluid having a different density or, if stratified, being characterized by a z-dependent ambient density. When the gate is rapidly extracted the lock-fluid collapses and propagates horizontally into the ambient.

Although most studies have involved a uniform-density ambient, an increasing number of full-depth lock-release experiments have been performed to examine the evolution of intrusions in stratified fluids. Most of these have focused upon the evolution of a so-called "symmetric" intrusion whose density if the average ambient density and the ambient itself is either a two-layer fluid with a thin or thick interface or a uniformly stratified fluid.[8–12] The evolution of asymmetric intrusions (having density different from the average ambient density) has been examined recently in full-depth lock release experiments with two-layer and continuously stratified ambients.[13–17]

Less is known about the evolution of intrusions in uniformly stratified fluid resulting from the collapse of partially mixed regions. The collapse of localized mixed patches at the mid-depth thick-interface two-layer fluids and in uniformly stratified fluids has been examined in experiments in which fluid is injected or transiently mixed at by a set of rollers or an oscillating grid.[18–22] In particular, through the displacement of horizontal dye lines Wu[18] observed that the collapsing intrusion generated vertically propagating internal waves in uniformly stratified fluid.

A study into the collapse of a partially mixed region, which is more readily amenable to theoretical and numerical modelling is set up so that the intrusion is instantaneously released from a lock whose depth spans only a fraction of the full depth of the tank. Such partial-depth lock-release experiments in nonuniformly stratified fluid were performed by Flynn and Sutherland[23] and Sutherland *et al.*,[24] who examined the propagation of an intrusion along the interface between a uniform-density and uniformly stratified fluid. These circumstances were designed to represent an idealization of the propagation of thunderstorm outflows below the tropopause or of an intrusion overriding a thermocline. The studies showed that the intrusion excited vertically propagating internal gravity waves in the stratified fluid layer and that the

[a]Author to whom correspondence should be addressed.

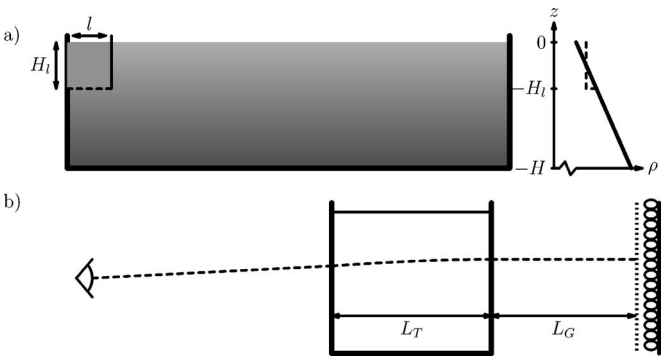

FIG. 1. Schematic of experimental setup showing (a) front view of tank with uniformly stratified ambient (solid line in right-hand density profile plot) and near surface mixed layer (dashed line). (b) Side view showing measurement of wave characteristics using synthetic schlieren.

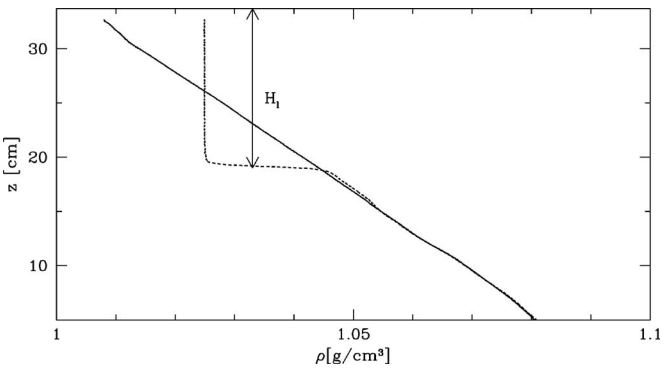

FIG. 2. Density profiles of the ambient (solid line) and lock fluid (dashed line) measured in an experiment with $N \simeq 1.63\ s^{-1}$ and $H_\ell \simeq 14.7$ cm, as indicated.

momentum transport associated with the waves could be substantial, although this depended upon the flow speed.

Rather than examining intrusions immediately above or below a stratified region, this study examines the collapse of a vertically and horizontally localized mixed patch into a uniformly stratified ambient. Over the vertical extent of the mixed patch, the system is similar to that studied by Munroe *et al.*[17] in that the patch collapses, intruding horizontally into the ambient and exciting internal wave modes in the ambient over the vertical extent of the patch. In the circumstance examined here, however, there is no solid boundary below the mixed region. As a result, the modes and the motion of the intrusion itself can excite internal waves that propagate vertically downward away from the horizontally spreading intrusion.

Unlike the dye-line technique of Wu,[18] here the frequency, horizontal wavenumber, and amplitude of vertically propagating internal waves are determined using a nonintrusive laboratory technique called synthetic schlieren.[25] Their associated energy is compared with the available potential energy associated with the initial state in order to determine how the intrusion and associated return flows leak energy into vertically propagating internal waves below this layer.

The experimental setup and schlieren analysis methods are discussed in Sec. II. Quantitative analyses of results is provided in Sec. III. Finally, in Sec. IV, we consider the application of these results to deep ocean mixing.

II. EXPERIMENTAL SETUP

The experiments were performed in a rectangular glass tank which is 197.1 cm long, 48.5 cm tall, and 17.4 cm wide. Using the standard "double bucket" technique,[26] the tank was filled with room-temperature salt-stratified fluid to a total depth H, as indicated in Fig. 1(a). Typically $H \sim 33$ cm.

Using a vertically traversing conductivity probe (Precision Measurement Engineering), it was confirmed that the ambient fluid was uniformly stratified. Finding a best-fit line through the density profile gave an accurate measure of the density gradient from which the buoyancy frequency was determined. The stratification was varied so that the buoyancy frequency ranged between $N \sim 0.7$ and $1.9\ s^{-1}$.

Once filled, an acrylic gate spanning the width of the tank was inserted between a pair of glass guides. These ensured that the gate would be extracted vertically when releasing the lock fluid. Exclusively, the length of the lock was $\ell = 18.5$ cm. The gate was inserted to a depth moderately greater than H_ℓ, which is the depth to be established for the mixed region. A mixer, a spiral horizontal disk that rotates back and forth, was inserted and operated between 5 and 30 s until the desired mixed depth was established.

The conductivity probe traversed through the lock fluid and underlying ambient in order to measure the density profile. This is illustrated schematically as the dotted line in the right plot of Fig. 1(a). Experiments were performed and analyzed only if the resulting density profile exhibited a uniform density region of depth $H_\ell > 3$ cm below the surface. Figure 2 shows typical density profiles measured in an experiment. The ambient density profile increases linearly with depth where as the density profile taken through the lock fluid after mixing shows that the fluid has uniform density over a depth H_ℓ and is separated from the stratified ambient beneath by a relatively thin interface.

To measure the depth H_ℓ, the maximum density gradient associated with the mid-depth of the interface was determined. From this the level of the interface mid-depth, z_i and the half-thickness, σ_i, of the interface was determined. The extent of the uniform-density fluid was thus defined to be $H_\ell = H - (z_i + \sigma_i)$.

Synthetic schlieren[25] was used to visualize and measure the amplitude of the vertically propagating waves. The setup is illustrated in Fig. 1(b). A 40 cm×40 cm grid of horizontal black and white lines each 3 mm thick was placed 18 cm behind the tank with its left-hand side at the position of the gate. A digital camera was situated on the opposite side of the tank and looked horizontally through it at the image of lines. The camera was positioned 300 cm from the tank and was zoomed in so that the image filled the field-of-view. Thus the effects of parallax were reduced.

Schlieren works by taking advantage of the fact that light bends to a greater degree as it passes through saltier water. As vertical density gradients increase due to the com-

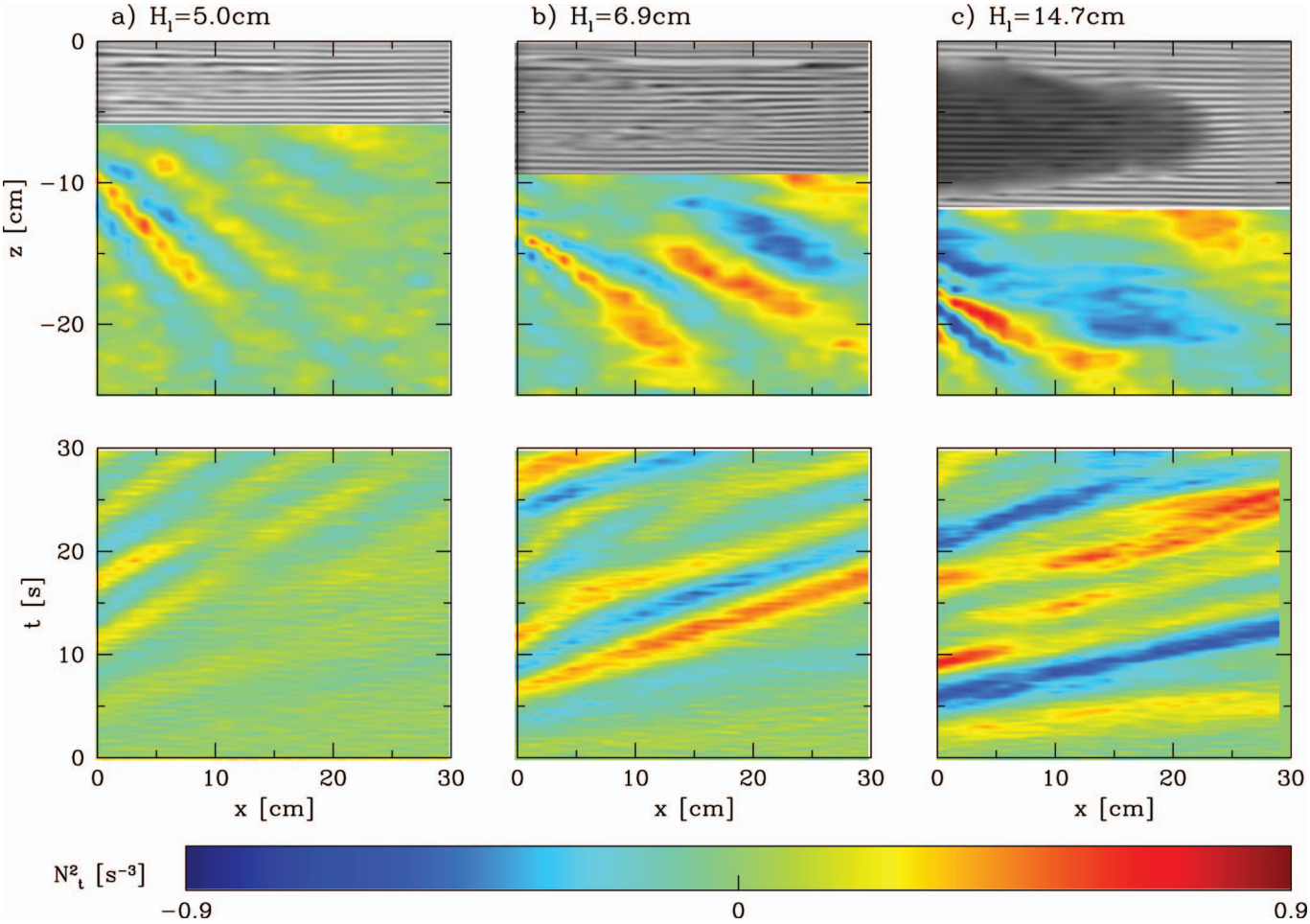

FIG. 3. (Color) Results of three experiments with (a) $H_\ell = 5.0$ cm, (b) 6.7 cm, and (c) 14.7 cm, as indicated. In each case the top plots show a composite snapshot composed of the raw image of horizontal lines and the color image showing the computed values of N_t^2; the bottom row plots horizontal time series of N_t^2 taken 10 cm below H_ℓ. In all cases $z=0$ corresponds to the surface of the fluid, $x=0$ corresponds to the position of the gate and $t=0$ corresponds to the time at which the gate is extracted. The intrusion is visualized by distortions of the black and white lines in (a) and (b) and is more clearly visualized by dye in (c). Values of N_t^2 are indicated by the color scale below the plots (enhanced online).

pression of isopycnal surfaces by waves, light rays bend further downward and locally the image appears to displace upwards. Conversely the image appears to shift downwards where internal waves stretch isopycnal surfaces apart. By recording the apparent displacement of the lines in the image and, assuming that the disturbances in the tank are spanwise-uniform, the vertical density gradient field, $\partial_z \rho$, was measured nonintrusively. For conceptual convenience this is multiplied by $-g/\rho_0$ to give $\Delta N^2 = -(g/\rho_0)\partial\rho/\partial z$, which is the change in the squared buoyancy frequency due to waves.

Often it is useful instead to measure changes in ΔN^2 between small times and to estimate the time derivative $N_t^2 \equiv \partial \Delta N^2/\partial t$. Measuring this field has the advantage over measuring ΔN^2 in that it filters long time-scale variations and enhances relatively fast time-scale internal waves. Furthermore, this field is found to be proportional to the vertical displacement field, ξ. Using estimates based on linear theory, the amplitude of vertical displacements due to waves can be determined and compared with the horizontal wavelength in order to provide an intuitive estimate of the height of the internal waves.

Like the waves, the intrusion was visualized by the distortion of the background image. Though too turbulent, and hence nonspanwise uniform, to enable the measurement of perturbation density gradients, its motion and extent can nonetheless be tracked. A single snapshot is not always clearly revealing, but the motion is easily seen in movie images. In some circumstances, dye is added to the mixed patch in the lock before it is released to allow for easier visualization.

Figure 3 shows typical images used for the analysis. The six images were constructed for three different experiments, all with $N \simeq 1.9\ \mathrm{s}^{-1}$ and with H_ℓ holding three different values. For the experiment with $H_\ell \simeq 5.0$ cm, Fig. 3(a) shows a snapshot of the experiment taken after the intrusion has propagated more than halfway across the field of view (top). This plot is a composite showing above the image of the black and white lines behind the tank, which is distorted as a result of the intrusion moving in front of it, and showing below a color field representing values of N_t^2. This field is proportional to the vertical displacement of fluid due to internal waves. Waves are clearly seen to emanate downward and to the right.

Beneath this image is the corresponding horizontal time

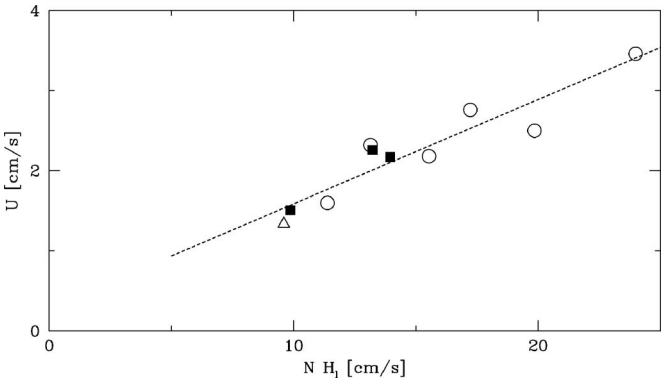

FIG. 4. Intrusion speed, U, plotted against NH_ℓ for $H_\ell < 5$ cm (open triangle), 5 cm $\leq H_\ell < 10$ cm (closed squares), and $H_\ell > 10$ cm (open circles). The dashed line indicates the best-fit line to the data with slope 0.13(±0.02).

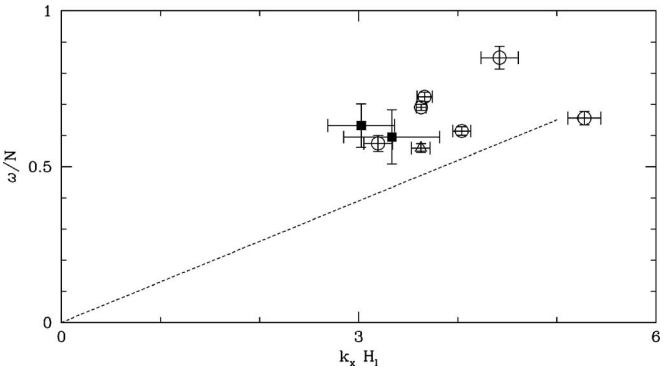

FIG. 5. Relative wave frequency plotted against the horizontal wavenumber with symbols plotted as indicated in the caption of Fig. 4. Error bars are indicated for each point. A dashed line is plotted with the same slope as the best-fit line shown in Fig. 4.

series constructed from a horizontal slice taken 10 cm below the base of the mixed region where $z=-H_\ell=-5.0$ cm. [That is, the horizontal slice in Fig. 3(a) is taken at $z=-15$ cm.] This shows that the waves move rightward, as expected. The image can be used to extract information on the phase speed, frequency, and horizontal wavenumber of the waves, as discussed in the next section.

In comparison, the top plots of Figs. 3(a)–3(c) show that the phase lines of the waves in all three cases tilt at approximately the same angle to the vertical. Because the buoyancy frequency is approximately the same in all three experiments, linear theory implies that the wave frequency is comparable in all three cases.

From horizontal time series images, as shown in the middle row of Fig. 3, we determine the horizontal phase speed of the waves by determining the best-fit line to constant-phase contours of the leading wave front. Likewise, from horizontal time series taken at a vertical level corresponding to the mid-depth of the mixed region (not shown), we determine the speed of the intrusion.

The horizontal time series are also used to estimate the frequency of the waves and this, combined with the phase speed, gives the horizontal wavenumber, k_x.

The amplitude of the waves, measured in terms of the N_t^2 field, is determined by computing the root-mean-square temporal average of the field measured from horizontal time series taken 10 cm below the mixed region. Taking the maximum result and multiplying by $2^{1/2}$ gives the amplitude, $A_{N_t^2}$, of the N_t^2 field. Linear theory is then used to estimate the amplitude of the vertical displacement field, A_ξ,

$$A_\xi = (N^3 k_x \sin\Theta)^{-1} A_{N_t^2}, \tag{1}$$

in which $\Theta \equiv \cos^{-1}(\omega/N)$, a measure of the relative wave frequency, is the angle at which lines of constant phase are oriented with the vertical.

III. RESULTS

First we examine the propagation of the intrusion. Figure 4 plots the measured horizontal speed of the intrusion, U, against the characteristic velocity scale NH_ℓ. The best-fit line through the data has slope 0.13±0.02, which is consistent with the results of Munroe and Sutherland,[17] who found that an intrusion released from a full-depth lock and which propagated at mid-depth in uniformly stratified fluid has speed moderately less than the two-layer theory prediction that $U/NH \lesssim 1/(4\sqrt{2}) \simeq 0.18$. The small correction was attributed to energy loss through internal wave generation in the ambient. In the experiments reported upon here, the smaller speed could also be attributed in part to the extraction of the gate from a relatively small lock.

This result demonstrates that the intrusion released from a mixed patch of depth H_ℓ behaves as though it was released from a full depth lock in a tank of total depth H_ℓ. The presence of a stratified lower boundary rather than a rigid solid boundary does not affect the advance of the intrusion.

Nonetheless, the lower boundary was not rigid, and the advance of the intrusion together with its associated return flows deforms the isopycnal surfaces at the level of the base of the mixed region. Consequently, this can excite vertically propagating internal waves in the otherwise quiescent stratified fluid below the level of the mixed region.

Figure 5 shows the measured characteristics of the waves. The frequency and horizontal wavenumber are determined from horizontal time series such as those shown in Fig. 3. Although there is some scatter in data, generally we find that the nondimensional frequency and horizontal wavenumber lie in a relatively narrow range. In particular, for experiments with N ranging from 0.7 to 1.9 s^{-1}, we find that the relative frequency, ω/N, lies between 0.6 and 0.8. Likewise, although H_ℓ ranges from 3.5 to 15.4 cm, the relative horizontal wavenumber, $k_x H_\ell$, lies between 3 and 5.

The dashed line superimposed on the plot passes through the origin having the same slope as the best-fit line shown in Fig. 4. If the speed of the intrusion set the horizontal phase speed, $c_p = \omega/k_x$, of the internal waves, the points would fall on this line. That this does not occur demonstrates that the intrusion speed does not establish the time scale for vertically propagating internal waves. Rather it is a combination of the buoyancy frequency setting ω and the mixed-region depth setting k_x.

That internal waves are generated in a narrow relative frequency range by a fluidic source is surprising but not new. Such observations have been made for waves generated by

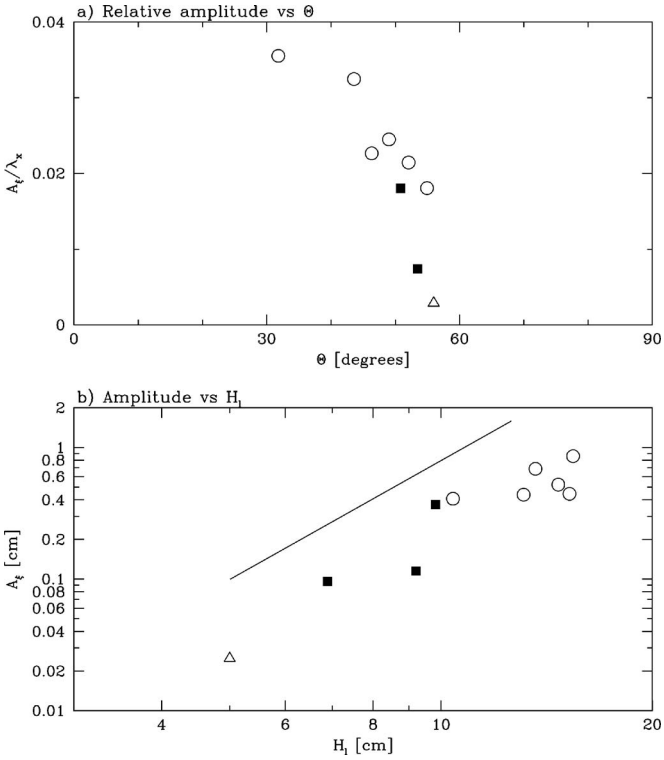

FIG. 6. (a) Measured relative vertical displacement amplitude of waves, A_ξ/λ_x, plotted against $\Theta \equiv \cos^{-1}(\omega/N)$. The convention for defining the symbols is given in the caption of Fig. 4. (b) Log-log plot of A_ξ vs H_ℓ. The solid line has a slope of 3.

stationary turbulence in mixing-box experiments,[27,28] by turbulence in the lee of obstacles,[29–32] and by collapsing mixed regions in uniformly stratified fluid.[17] This phenomenon has likewise been reproduced recently in numerical simulations.[33,34]

Although a definitive explanation remains elusive at this time, the fact that their frequency is close to that of waves that transport energy and momentum with the greatest flux ($35° \lesssim \Theta \lesssim 45°$) suggests that enhanced generation of these waves results from resonant interactions between the waves and their source. This hypothesis seems more reasonable in light of the fact that the waves are generated at relatively large amplitudes, as shown in Fig. 6.

Figure 6(a) shows that, relative to the horizontal wavelength, the vertical displacement amplitude of the waves can be as large as 4%, well into the range at which the waves exhibit weakly nonlinear behavior.[35,36] The relative amplitude increases with increasing H_ℓ.

The amplitude itself increases with increasing H_ℓ. Figure 6(b) shows a log-log plot of A_ξ and H_ℓ. The vertically offset line has slope 3. The best-fit line through all the data gives a power law exponent of 2.8 ± 0.3, although the actual power law behavior has moderately larger exponent for small H_ℓ and smaller exponent for $H_\ell \gtrsim 10$ cm. A cubic power law can be explained in terms of the pressure perturbation exerted at the top of the quiescent stratified region below the collapsing mixed region. The horizontal motion resulting from the return flow scales linearly with H_ℓ and so the corresponding pressure perturbation, being proportional to speed squared, scales as H_ℓ^2. But there is an additional pressure perturbation due to the vertical flow around the intrusion head. The low pressure in the lee of the head has magnitude proportional to the head height, which is itself proportional to H_ℓ. Thus the total pressure perturbation at the top of the quiescent fluid, and hence the amplitude of the launched waves, is proportional to H_ℓ^3.

Though exhibiting power law behavior at low H_ℓ, the amplitude cannot grow without bound. Weakly nonlinear effects become significant if A_ξ is larger than about 1% of the horizontal wavelength.[36] These effects act to enhance the dispersion of the waves and can lead to wave breaking; although such breaking was not observed in the experiments. In their observed frequency range, the waves are overturning if A_ξ is moderately larger than 10% of the horizontal wavelength.[35]

IV. DISCUSSION AND CONCLUSIONS

We have examined the properties of vertically propagating internal waves generated by the collapse of a vertically and horizontally localized mixed patch. The waves were found to have frequencies dominantly between 0.5 and 0.7N. The horizontal and vertical wavelengths are therefore comparable and increase with the depth, H_ℓ, of the mixed layer so that $H_\ell \lesssim \lambda_x, \lambda_z \lesssim 1.5 H_\ell$. The vertical displacement amplitude increases approximately as the cube of the mixed layer depth for low H_ℓ. The amplitude must be limited, however, because the waves approach breaking amplitudes if A_ξ/λ_x is approximately 0.1.

Given the characteristics of the waves, we may estimate their associated energy. From linear theory, the vertical energy flux per unit horizontal wavelength of monochromatic internal waves is

$$\langle \mathcal{F} \rangle = \tfrac{1}{2} \varrho_0 (N/k_x)^3 \sin\Theta \cos^2\Theta (k_x A_\xi)^2. \tag{2}$$

For saturated wave amplitudes, having $k_x A_\xi \simeq 0.2$, taking $\Theta = 45°$ and $k_x \simeq 4/H_\ell$, this gives the estimate $\langle \mathcal{F} \rangle \simeq 1 \times 10^{-4} \varrho_0 (N H_\ell)^3$.

Based on images like those in Fig. 3, we suppose the intrusion excites wavepackets over two buoyancy periods and that the waves extract energy uniformly over the half-depth $H_\ell/2$ of the mixed region. Then the loss of energy density per unit mass in the mixed region associated with extraction by vertically propagating waves is

$$E_{\text{wave}} \simeq 0.003 (N H_\ell)^2. \tag{3}$$

This quantity is compared with the available potential energy density per unit mass of the system before the gate is extracted. This is given by[17]

$$E_{\text{init}} = \tfrac{1}{24} (N H_\ell)^2 \simeq 0.04 (N H_\ell)^2. \tag{4}$$

Thus almost 10% of the energy associated with the lock fluid is extracted by waves.

It is tempting to extend these results to estimate the characteristics of waves generated from a mixed region in the ocean. Using the observed data by Gregg,[4] we assume the storm uniformly mixes the near-surface of the ocean down to a depth of 100 m and that the surrounding stratification is

approximately uniform with $N \simeq 0.007\ s^{-1}$. The resulting collapse of the region should excite nonhydrostatic internal waves with frequencies comparable to the background buoyancy frequency, about $0.005\ s^{-1}$, and with wavelengths on the order of 100 m. The waves should be generated at large amplitude having maximum vertical displacements no larger than 10 m.

Nonlinear effects either would lead to breaking or would act rapidly to disperse the waves through interactions with the wave-induced mean flow and transfer their energy to smaller scales through parametric subharmonic instability.[37] Based on simulations by Sutherland,[38] this would happen within a few buoyancy periods and so would not likely be observed except by *in situ* probes during the passage of a storm itself.

ACKNOWLEDGMENTS

This work has been supported by the Natural Sciences and Engineering Research Council of Canada (NSERC), the Canadian Foundation for Climate and Atmospheric Science (CFCAS), and the Alberta Ingenuity Studentship program.

[1] A. E. Gill, *Atmosphere-Ocean Dynamics* (Academic San Diego, 1982).
[2] K. E. Brainerd and M. C. Gregg, "Surface mixed and mixing layer depths," Deep-Sea Res., Part I **42**, 1521 (1995).
[3] R. Ferrari and W. R. Young, "On the development of thermohaline correlations as a result of nonlinear diffusive parameterizations," J. Mar. Res. **55**, 1069 (1997).
[4] M. C. Gregg, "Fine structure and microstructure observations during the passage of a mild storm," J. Phys. Oceanogr. **6**, 528 (1976).
[5] S. A. Thorpe, "The excitation, dissipation, and interaction of internal waves in the deep ocean," J. Geophys. Res. **80**, 328 (1975).
[6] J. E. Simpson, "Gravity currents in the laboratory, atmosphere, and ocean," Annu. Rev. Fluid Mech. **14**, 213 (1982).
[7] J. E. Simpson, *Gravity Currents*, 2nd ed. (Cambridge University Press, Cambridge, 1997).
[8] R. E. Britter and J. E. Simpson, "A note on the structure of the head of an intrusive gravity current," J. Fluid Mech. **112**, 459 (1981).
[9] K. M. Faust and E. J. Plate, "Experimental investigation of intrusive gravity currents entering stably stratified fluids," J. Hydraul. Res. **22**, 315 (1984).
[10] R. J. Lowe, P. F. Linden, and J. W. Rottman, "A laboratory study of the velocity structure in an intrusive gravity current," J. Fluid Mech. **456**, 33 (2002).
[11] A. Mehta, B. R. Sutherland, and P. J. Kyba, "Interfacial gravity currents. II. Wave excitation," Phys. Fluids **14**, 3558 (2002).
[12] B. R. Sutherland and J. T. Nault, "Intrusive gravity currents propagating along thin and thick interfaces," J. Fluid Mech. **586**, 109 (2007) .
[13] B. R. Sutherland, P. J. Kyba, and M. R. Flynn, "Interfacial gravity currents in two-layer fluids," J. Fluid Mech. **514**, 327 (2004).
[14] H.-B. Cheong, J. J. P. Kuenen, and P. F. Linden, "The front speed of intrusive gravity currents," J. Fluid Mech. **552**, 1 (2006).
[15] M. R. Flynn and P. F. Linden, "Intrusive gravity currents," J. Fluid Mech. **568**, 193 (2006).
[16] D. Bolster, A. Hang, and P. F. Linden, "The front speed of intrusions into a continuously stratified medium," J. Fluid Mech. (in press).
[17] J. R. Munroe and B. R. Sutherland, "Intrusions and internal waves in stratified fluids," in *Proceedings of the Sixth International Symposium on Stratified Flows*, edited by G. N. Ivey (IAHR University of Western Australia, 2006), pp. 446–451.
[18] J. Wu, "Mixed region collapse with internal wave generation in a density stratified medium," J. Fluid Mech. **35**, 531 (1969).
[19] A. H. Schooley and B. A. Hughes, "An experimental and theoretical study of internal waves generated by the collapse of a two-dimensional mixed region in a density gradient," J. Fluid Mech. **51**, 159 (1972).
[20] P. C. Manins, "Intrusion into a stratified fluid," J. Fluid Mech. **74**, 547 (1976).
[21] I. P. D. De Silva and H. J. S. Fernando, "Experiments on collapsing turbulent regions in stratified fluids," J. Fluid Mech. **358**, 29 (1998).
[22] V. S. Maderich, G. J. F. van Heijst, and A. Brandt, "Laboratory experiments on intrusive flows and internal waves in a pycnocline," J. Fluid Mech. **432**, 285 (2001).
[23] M. R. Flynn and B. R. Sutherland, "Intrusive gravity currents and internal wave generation in stratified fluid," J. Fluid Mech. **514**, 355 (2004).
[24] B. R. Sutherland, M. R. Flynn, and K. Dohan, "Internal wave excitation from a collapsing mixed region," Deep-Sea Res., Part II **51**, 2889 (2004).
[25] B. R. Sutherland, S. B. Dalziel, G. O. Hughes, and P. F. Linden, "Visualisation and measurement of internal waves by 'synthetic schlieren.' Part 1: Vertically oscillating cylinder," J. Fluid Mech. **390**, 93 (1999).
[26] G. Oster, "Density gradients," Sci. Am. **213**, 70 (1965).
[27] P. F. Linden, "The deepening of a mixed layer in a stratified fluid," J. Fluid Mech. **71**, 385 (1975).
[28] K. Dohan and B. R. Sutherland, "Internal waves generated from a turbulent mixed region," Phys. Fluids **15**, 488 (2003).
[29] B. R. Sutherland and P. F. Linden, "Internal wave generation by flow over a thin barrier," J. Fluid Mech. **377**, 223 (1998).
[30] B. R. Sutherland, "Large-amplitude internal wave generation in the lee of step-shaped topography," Geophys. Res. Lett. **29**, 1769, DOI:10.1029/2002GL015321 (2002).
[31] D. A. Aguilar, B. R. Sutherland, and D. J. Muraki, "Generation of internal waves over sinusoidal topography," Deep-Sea Res., Part II **53**, 96 (2006).
[32] D. A. Aguilar and B. R. Sutherland, "Internal wave generation from rough topography," Phys. Fluids **18**, 066603 (2006).
[33] P. J. Diamessis, J. A. Domaradzki, and J. S. Hesthaven, "A spectral multidomain penalty method model for the simulation of high Reynolds number localized incompressible stratified turbulence," J. Comput. Phys. **202**, 298 (2005).
[34] J. R. Taylor and S. Sarkar (private communication, 2007).
[35] B. R. Sutherland, "Finite-amplitude internal wavepacket dispersion and breaking," J. Fluid Mech. **429**, 343 (2001).
[36] B. R. Sutherland, "Weakly nonlinear internal wavepackets," J. Fluid Mech. **569**, 249 (2006).
[37] P. N. Lombard and J. J. Riley, "On the breakdown into turbulence of propagating internal waves," Dyn. Atmos. Oceans **23**, 345 (1996).
[38] B. R. Sutherland, "Internal wave instability: Wave-wave vs wave-induced mean flow interactions," Phys. Fluids **18**, 074107 (2006).